Boundary-Layer Meteorology (2006) 119: 397–407
DOI 10.1007/s10546-005-9030-8

AN IMPROVED MELLOR–YAMADA LEVEL-3 MODEL: ITS NUMERICAL STABILITY AND APPLICATION TO A REGIONAL PREDICTION OF ADVECTION FOG

MIKIO NAKANISHI[1,*] and HIROSHI NIINO[2]
[1]*National Defence Academy, Yokosuka, Kanagawa 239-8686, Japan;* [2]*Ocean Research Institute, The University of Tokyo, Nakano, Tokyo 164-8639, Japan*

(Received in final form 18 September 2005 / Published online: 14 March 2006)

Abstract. This note describes a numerically stable version of the improved Mellor–Yamada (M–Y) Level-3 model proposed by Nakanishi and Niino [Nakanishi, M. and Niino, H.: 2004, *Boundary-Layer Meteorol.* **112**, 1–31] and demonstrates its application to a regional prediction of advection fog. In order to ensure the realizability for the improved M–Y Level-3 model and its numerical stability, restrictions are imposed on computing stability functions, on L/q, the temperature and water-content variances, and their covariance, where L is the master length scale and $q^2/2$ the turbulent kinetic energy per unit mass. The model with these restrictions predicts vertical profiles of mean quantities such as temperature that are in good agreement with those obtained from large-eddy simulation of a radiation fog. In a regional prediction, it also reasonably reproduces the satellite-observed horizontal distribution of an advection fog.

Keywords: Advection fog, Level-3 model, Realizability, Regional prediction, Turbulence closure model.

1. Introduction

Nakanishi (2001) and Nakanishi and Niino (2004, hereafter NN04) proposed an improved Mellor–Yamada (M–Y) Level-3 model on the basis of large-eddy simulation (LES) data. Using this model, we have recently attempted three-dimensional simulations of advection fog. During the simulations, the model showed problems that seem to be due to a computational instability.

Higher-order turbulence closure models are known to behave often pathologically. The principal cause for this is that these models do not always satisfy realizability conditions: e.g., a constraint that velocity variances remain non-negative. To ensure the realizability for the M–Y Level-2.5

* E-mail: naka@nda.ac.jp

model, many researchers have suggested inclusion of various restrictions and modifications on parameters involving velocity and temperature gradients and on the turbulent kinetic energy (TKE) and length scale (e.g., Mellor and Yamada, 1982, hereafter MY82; Galperin et al., 1988; Helfand and Labraga, 1988, hereafter HL88; Gerrity et al., 1994; Janjić, 2001). Our improved M–Y Level-3 model is incorporated with the modification by HL88, which appears to be physically most plausible. Since HL88 did not consider the realizability for a Level-3 model, however, the above problems of the improved M–Y Level-3 model may imply the necessity of an additional modification.

The first aim of the present paper is to describe a scheme for imposing several restrictions on turbulent quantities such as temperature variance in order to ensure the realizability for the improved M–Y Level-3 model and its numerical stability (Section 2). The second is to demonstrate an application of the model with the restrictions to a regional prediction of advection fog around northern Japan (Section 3).

2. Improved Mellor–Yamada Level-3 Model and Restrictions

2.1. Stability functions

The improved M–Y Level-3 model is described in NN04, to which the readers may refer. According to NN04, the stability functions, S_M and S_H, in the turbulent-diffusivity coefficients for the Level-3 model are written as

$$S_M = S_{M2.5} + S'_M = \frac{R_1 E_4 - R_2 E_2}{E_1 E_4 - E_2 E_3} - \frac{R'_2 E_2}{E_1 E'_4 - E_2 E_3}, \tag{1a}$$

$$S_H = S_{H2.5} + S'_H = \frac{R_2 E_1 - R_1 E_3}{E_1 E_4 - E_2 E_3} + \frac{R'_2 E_1}{E_1 E'_4 - E_2 E_3}, \tag{1b}$$

where the subscript 2.5 denotes a variable in the Level-2.5 model, a prime the difference from it, and E and R with subscripts are defined in NN04.

According to HL88, the denominators, $D_{2.5}$ and D', of the first and second terms on the right-hand side of Equations (1a) and (1b) can be rewritten as

$$D_{2.5} \equiv E_1 E_4 - E_2 E_3 = \Phi_2 \Phi_4 + (1-\alpha)^2 6 A_1^2 G_M \Phi_3, \tag{2a}$$

$$D' \equiv E_1 E'_4 - E_2 E_3 = \Phi_2 \Phi'_4 + (1-\alpha)^2 6 A_1^2 G_M \Phi'_3, \tag{2b}$$

with

$$\Phi_1 = 1 - (1-\alpha)^2 3 A_2 B_2 (1 - C_3) G_H = 1 - (1-\alpha)^2 20.3 G_H, \tag{3a}$$

$$\Phi_2 = 1 - (1-\alpha)^2 9 A_1 A_2 (1 - C_2) G_H = 1 - (1-\alpha)^2 2.12 G_H, \tag{3b}$$

$$\Phi_3 = \Phi_1 + (1-\alpha)^2 9 A_2^2 (1 - C_2)(1 - C_5) G_H = 1 - (1-\alpha)^2 19.3 G_H, \tag{3c}$$

$$\Phi_3' = 1 + (1-\alpha)^2 9 A_2^2 (1 - C_2)(1 - C_5) G_H = 1 + (1-\alpha)^2 0.955 G_H, \tag{3d}$$

$$\Phi_4 = \Phi_1 - (1-\alpha)^2 12 A_1 A_2 (1 - C_2) G_H = 1 - (1-\alpha)^2 23.1 G_H, \tag{3e}$$

$$\Phi_4' = 1 - (1-\alpha)^2 12 A_1 A_2 (1 - C_2) G_H = 1 - (1-\alpha)^2 2.82 G_H, \tag{3f}$$

$$G_M = \frac{L^2}{q^2}\left[\left(\frac{\partial U}{\partial z}\right)^2 + \left(\frac{\partial V}{\partial z}\right)^2\right], \tag{4a}$$

$$G_H = -\frac{L^2}{q^2}\frac{g}{\Theta_0}\left(\beta_\theta \frac{\partial \Theta_l}{\partial z} + \beta_q \frac{\partial Q_w}{\partial z}\right), \tag{4b}$$

where α $(0 \le \alpha \le 1)$ is a function introduced by HL88 in order to ensure the realizability for the Level-2.5 model in the case of growing turbulence, A, B, and C with subscripts are closure constants (NN04), (U, V) the velocity components of the horizontal wind, Θ_l is the liquid-water potential temperature, Q_w the total-water content, $q^2/2$ the TKE per unit mass, L the master length scale, Θ_0 the potential temperature in a reference state, g the gravitational acceleration, and β_θ and β_q are functions determined from the condensation process (NN04).

Both the denominators $D_{2.5}$ and D' are positive under neutral stratification ($G_H = 0$), since $\Phi_2 = \Phi_3 = \Phi_3' = \Phi_4 = \Phi_4' = 1$ and $(1-\alpha)^2 6 A_1^2 G_M \ge 0$. If $D_{2.5}$ and D' should become negative for changing G_H with stability, they would vanish at a certain value of G_H. In the following subsection we shall demonstrate that, to keep $D_{2.5}$ and D' positive and avoid such a singularity, several restrictions need to be introduced.

2.2. Restriction on L/q

2.2.1. *Unstable Stratification*

Since $G_H > 0$ for unstable stratification, Φ_2, Φ_3, Φ_4, and consequently $D_{2.5}$ can become non-positive. Because the Level-2 model is non-singular, such a singularity is found to occur when G_H (q^2) is larger (smaller) than that in the Level-2 model, i.e., in the case of growing turbulence. To prevent this, a number of previous studies imposed restrictions on G_H, q^2, and L (e.g., MY82; Gerrity et al., 1994; Janjić, 2001). The function α introduced

by HL88 also substantially corresponds to a restriction on q^2 and assures the positiveness of the above quantities.

From Equations (2a) and (2b), $D' - D_{2.5}$ is obtained as

$$D' - D_{2.5} = \Phi_2(1-\alpha)^2 20.28 G_H + (1-\alpha)^2 6A_1^2 G_M 20.255 G_H. \tag{5}$$

Since $G_H > 0$ and α guarantees that $\Phi_2 > 0$ and $D_{2.5} > 0$ (HL88), D' is also positive. Thus, for unstable stratification, no additional restriction to HL88 is necessary to avoid the singularity.

2.2.2. *Stable Stratification*

Since Φ_2, Φ_3, and Φ_4 are positive for $G_H < 0$, $D_{2.5}$ remains positive. D', on the other hand, can become non-positive if Φ_3' is negative and G_M is large. A problem for stable stratification has been reported on the realizability of the vertical velocity variance (e.g., MY82; Janjić, 2001). However, the one associated with the singularity of D' has not been considered, because the previous studies have been confined to improving the stability of the Level-2.5 model.

Equation (3d) shows that, to ensure the positiveness of Φ_3' for any value of α, G_H must be larger than $-1/0.955 \approx -1$. Considering Equation (4b), we will therefore impose a restriction on L/q as

$$\frac{L}{q} \le \left[\frac{g}{\Theta_0} \left(\beta_\theta \frac{\partial \Theta_l}{\partial z} + \beta_q \frac{\partial Q_w}{\partial z} \right) \right]^{-1/2} \quad \text{for } G_H < 0. \tag{6}$$

If the vertical gradient of the virtual potential temperature, $\partial \Theta_V / \partial z$, is given by

$$\frac{\partial \Theta_V}{\partial z} = \beta_\theta \frac{\partial \Theta_l}{\partial z} + \beta_q \frac{\partial Q_w}{\partial z}, \tag{7}$$

this restriction means $L/q \le 1/N$ (or $L \le q/N$), where N is the Brunt–Väisälä frequency.

Under stable stratification, the master length scale L tends to be limited by the buoyancy length scale L_B. Nakanishi (2001) and NN04 adopted

$$L_B = \begin{cases} q/N, & \partial \Theta_V / \partial z > 0 \text{ and } \zeta \ge 0 \\ (1 + I_t) q/N, & \partial \Theta_V / \partial z > 0 \text{ and } \zeta < 0, \end{cases} \tag{8}$$

where $\zeta \equiv z/L_M$ with the Obukhov length L_M. Note that the first condition typically applies to a nocturnal boundary layer, while the second to the upper part of a convective mixed layer for which the increase of TKE, I_t, due to the turbulent transport and the buoyancy production is considered. It is found that Equation (6) is always satisfied for $\zeta \ge 0$, but not for $\zeta < 0$, so that a modification on L/q is made in the upper part of the mixed layer.

Note that this restriction on L/q is to be imposed only when G_M and G_H in the stability functions S_M and S_H are computed.

In NN04, different modifications of their Equations (26)–(30), in which E_4 (Φ_3) is approximated by E_4' (Φ_3'), were made to keep D' positive. Since the restriction on L/q ensures the positiveness of D', however, we no longer need to use their modifications. This gives a considerable simplification of Equations (31)–(34) in NN04; e.g., their Equation (31) becomes

$$\Gamma_\theta \equiv S_H' \frac{\partial \Theta_l}{\partial z} = E_H \frac{1}{q^2} \frac{g}{\Theta_0} (\langle \theta_l \theta_V \rangle - \langle \theta_l \theta_V \rangle_{2.5}), \tag{9}$$

where E_H and $\langle \theta_l \theta_V \rangle$ are defined in NN04.

2.3. Restrictions on variances

As stratification becomes stable and wind shear increases, the vertical velocity variance $\langle w^2 \rangle$ decreases. MY82 pointed out that the return-to-isotropy hypothesis of Rotta is valid in the range where all the normalized velocity variances are not less than 0.12, and imposed a lower bound of 0.12 only on $C_w \equiv \langle w^2 \rangle / q^2$. Janjić (2001) also considered a similar bound for C_w except that its value is about 0.14.

In the Level-3 model, the normalized velocity variances, C_w, $C_v \equiv \langle v^2 \rangle / q^2$, and $C_u \equiv \langle u^2 \rangle / q^2$, are expressed as

$$C_w = C_{w2.5} + C_w' = \frac{\Phi_1}{3} \frac{\Phi_2 + (1-\alpha)^2 18 A_1^2 C_1 G_M}{D_{2.5}} + \left[\frac{\Phi_2 + (1-\alpha)^2 6 A_1^2 G_M}{D'} - 1 \right] (1 - C_3) G_H (C_\theta - C_{\theta 2.5}), \tag{10a}$$

$$C_v = C_{v2.5} + C_v' = \frac{\Phi_5}{3} \frac{\Phi_2 + (1-\alpha)^2 18 A_1^2 C_1 G_M}{D_{2.5}} + \left[\Phi_5' \frac{\Phi_2 + (1-\alpha)^2 6 A_1^2 G_M}{D'} - 1 \right] (1 - C_3) G_H (C_\theta - C_{\theta 2.5}), \tag{10b}$$

$$C_u = C_{u2.5} + C_u' = (1 - C_{v2.5} - C_{w2.5}) - (C_v' + C_w'), \tag{10c}$$

where the directions of u and v are parallel and perpendicular to the mean flow, respectively, C_θ is the normalized temperature variance, $C_{\theta 2.5} = (1-\alpha) B_2 S_{H2.5}$, $\Phi_5 = \Phi_1 - (1-\alpha)^2 18 A_1 A_2 (1 - C_2) G_H$, and $\Phi_5' = 1 - (1-\alpha)^2 18 A_1 A_2 (1 - C_2) G_H$. These equations show that the large departure of C_θ from $C_{\theta 2.5}$ can reduce any of the normalized velocity variances to less than 0.12. Therefore we will impose the restrictions that $C_w \geq 0.12$, $C_v \geq 0.12$, and $C_u \geq 0.12$. Practically, these restrictions lead to restrictions on the temperature and water-content variances, $\langle \theta_l^2 \rangle$ and $\langle q_w^2 \rangle$, and their covariance

$\langle\theta_l q_w\rangle$; e.g., when multiplied by $L^2(\partial\Theta_l/\partial z)^2$, the restriction on C_w is converted into

$$F(1-C_3)G_H(\langle\theta_l^2\rangle - \langle\theta_l^2\rangle_{2.5}) \geq (0.12 - C_{w2.5})L^2\left(\frac{\partial\Theta_l}{\partial z}\right)^2, \tag{11}$$

where F is the quantity in the square brackets of Equation (10a).

Note that these restrictions are also imposed only when S_M and S_H are computed.

3. Simulations

3.1. One-dimensional simulation of a radiation fog

We first compare the performance of the improved M–Y Level-3 model with the present restrictions with that of the models in NN04 in a one-dimensional context. NN04 made a successful one-dimensional simulation of a radiation fog observed in The Netherlands (Musson-Genon, 1987) using their improved M–Y Level-3 model (Model I). The same fog is simulated here by the improved M–Y Level-3 model with the present restrictions (Model II). Figure 1 shows vertical profiles of temperature obtained from LES (thin lines; NN04), Model I, Model II, the improved Level-2.5 model (Model III; NN04), and the original Level-3 model of MY82 except that closure constants of Kantha and Clayson (1994) are used (Model O; NN04). NN04 has shown that Model I reproduces reasonably well the evolution of the mixed layer simulated by LES. Model II is found to give much better agreement with the temperature profiles simulated by LES; both the cold bias for the nocturnal boundary layer and the warm bias for the convective mixed layer almost disappear. This shows that the consideration of the limitations arising from model assumptions not only eliminates the inherent numerical instability but also returns a better performance.

Model III exhibits a fairly good performance comparable to Model II in the lower part of the mixed layer, but predicts a slower growth of the convective mixed layer. Note that Model O gives much worse prediction than Model III does.

3.2. Three-dimensional simulation of an advection fog

3.2.1. *Regional Prediction Model*

Model II is incorporated into a three-dimensional mesoscale hydrostatic model in the terrain-following coordinate system. The horizontal diffusivity coefficient K_h is given by

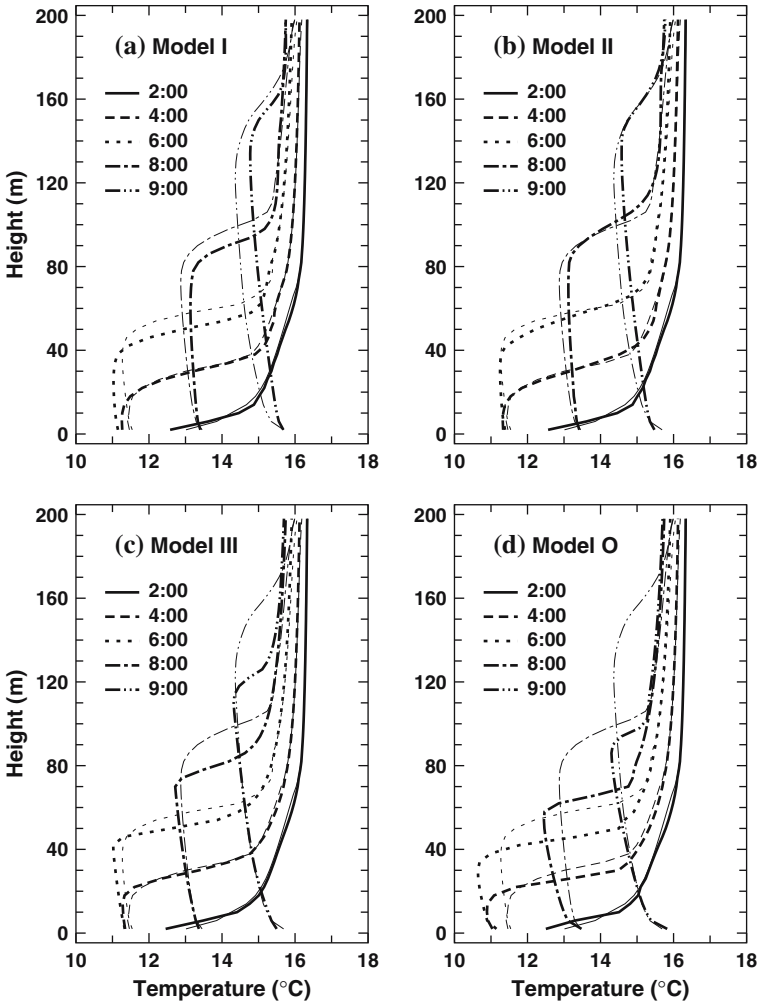

Figure 1. Vertical profiles of temperature obtained from (a) Model I (without the present restrictions), (b) Model II (with the present restrictions), (c) Model III, and (d) Model O. Solid, dashed, dotted, dot-dashed, and double dot-dashed lines represent the profiles at 0200, 0400, 0600, 0800, and 0900 UTC, respectively. Thin lines indicate LES results. All the results except those of Model II are extracted from Nakanishi and Niino (2004).

$$K_h = C_S^2 \Delta x \Delta y \left\{ 2 \left[\left(\frac{\partial U}{\partial x} \right)^2 + \left(\frac{\partial V}{\partial y} \right)^2 \right] + \left(\frac{\partial U}{\partial y} + \frac{\partial V}{\partial x} \right)^2 \right\}^{1/2}, \tag{12}$$

where Δx and Δy are horizontal grid spacings in the x- and y-directions, respectively, and C_S is chosen to be 0.4 (Smagorinsky et al., 1965). The lower-boundary conditions are determined from Monin–Obukhov similarity theory. The land-surface temperature is predicted by the force restore

method, while the sea-surface temperature (SST) is fixed at NEAR–GOOS daily SST provided by the Japan Meteorological Agency (JMA). The lateral-boundary condition is a radiative-nesting condition (Nakanishi, 2002). At the upper boundary, the radiative condition proposed by Klemp and Durran (1983) is imposed on the Exner pressure function to avoid reflections of gravity waves from the top boundary.

This three-dimensional model is used to simulate an advection fog that frequently appears around northern Japan in summer. The size of the computational domain is 920 km × 920 km in the horizontal directions and 5300 m in the vertical direction. The uniform horizontal grid spacing of 10 km is used, and the vertical grid spacing varies from 20 m near the surface to 400 m above a height of 3000 m. The model is one-way nested within the Regional Spectral Model (RSM; JMA, 2002), whose grid point values every 3 h are provided by JMA. A time step is set to 30 s.

3.2.2. *Results*

Figure 2a, b shows a visible image of GMS-5 at 1200 JST (Japan Standard Time; 0900 JST = 0000 UTC) on 5 August 1999 and a horizontal distribution of maritime winds from QuikSCAT at about 1800 JST on the same day, respectively. Warm, moist air advected by a southerly wind was cooled by the sea surface and eventually formed a fog layer over the Pacific near Hokkaido Island. Although the southerly wind was generally uniform over most of the computational domain, it was disturbed by the land effect around Hokkaido Island.

The simulation was started at 2100 JST on 4 August 1999 using the NEAR–GOOS daily SST on 5 August. Figure 2c, d shows horizontal distributions of liquid-water path (LWP) after 15 h and horizontal wind at 10-m height after 21 h, respectively. The characteristics of the wind field around Hokkaido Island are reproduced reasonably well (Figure 2b, d). The distribution of the fog over the Pacific is also in reasonable agreement with the satellite image, but that over the Sea of Okhotsk is erroneous (Figure 2a, c).

In order to examine the cause of this erroneous fog distribution over the Sea of Okhotsk, various sensitivity experiments were done. Among them, two of the significant experiments are shown in Figure 3. The first experiment called Experiment A is performed by replacing the SST with that on 10 August (Figure 3a). The NEAR–GOOS daily SST is analysed objectively from observations by satellites, ships, and buoys for the past 5 days. During several days before 5 August, a stationary front had existed over the Sea of Okhotsk, which may have disturbed the satellite observation. Since the SST of the Sea of Okhotsk on 10 August is evaluated to be about 1–2 K higher than that on 5 August, the fog over the Sea of Okhotsk is somewhat suppressed in Experiment A. Since the SST of the Pacific in the east of Hokkaido Island was about 0–3 K lower, on the other hand, the

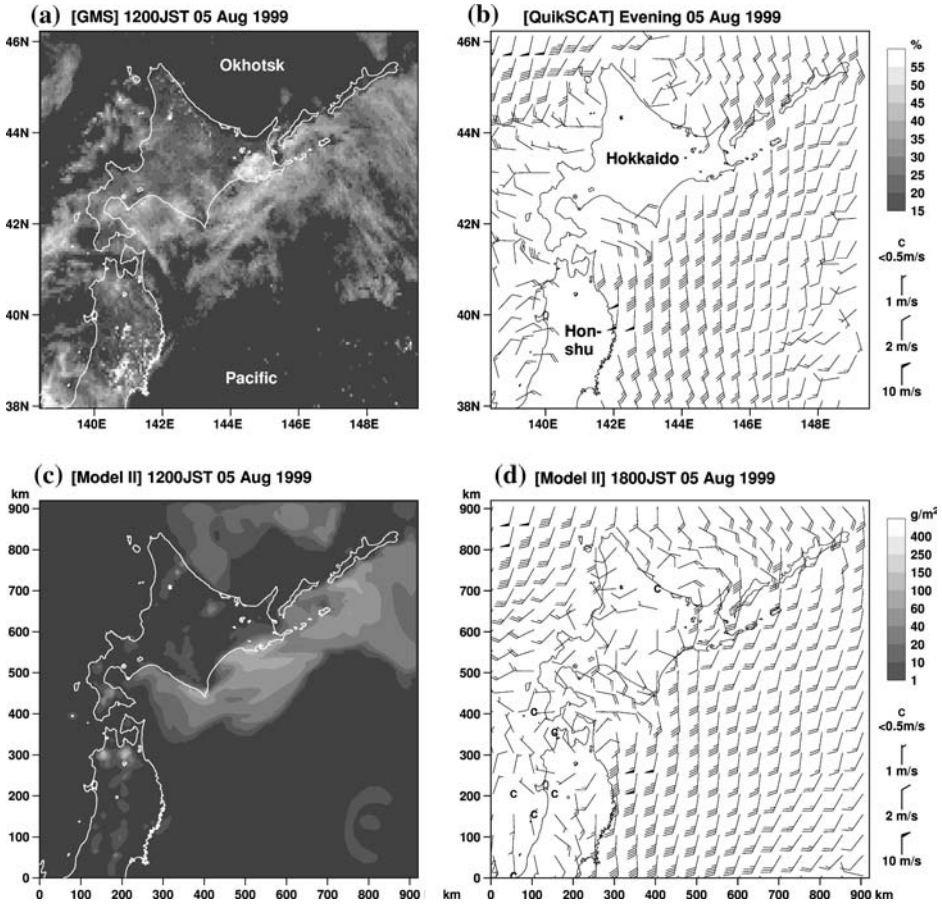

Figure 2. Horizontal distributions of (a) albedo (%) at 1200 JST from GMS-5, (b) maritime winds ($m\,s^{-1}$) at about 1800 JST from QuikSCAT, (c) LWP ($g\,m^{-2}$) at 1200 JST and (d) horizontal winds ($m\,s^{-1}$) at 10-m height at 1800 JST from Model II.

fog area over the Pacific expanded southward. These result in more resemblance to the satellite observation (Figure 2a).

The second experiment called Experiment B is performed by reducing the radiative heating/cooling rate by half (Figure 3b). For this experiment, the fog over the Sea of Okhotsk disappeared completely, although the fog area over the Pacific also was reduced. These two experiments show that, although SST is a factor affecting the formation of advection fog, the most important factor for the present case is the radiation process. Our radiation scheme is described in Nakanishi (2000) and NN04, in which the simplified longwave radiation scheme of Katayama (1972) is employed. We are planning to replace it with a more sophisticated scheme.

Finally, it should be mentioned that Model O with the present restrictions also predicts nearly a similar horizontal distribution of the fog (not

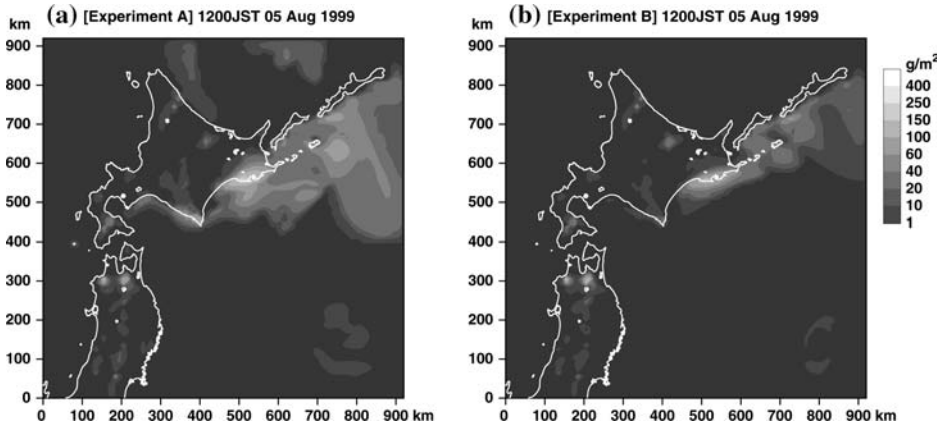

Figure 3. Horizontal distributions of LWP ($g\,m^{-2}$) at 1200 JST from (a) Experiment A and (b) Experiment B. From the control run in Figure 2c, Experiment A replaces the NEAR–GOOS daily SST on 5 August 1999 with that on 10 August 1999, and Experiment B reduces the radiative heating/cooling rate by half.

shown); however, Model O gives somewhat larger liquid-water content and thinner fog layer than Model II does, mainly because of the insufficient growth of the boundary layer in Model O. Since the liquid-water content and cloud-top height affect the shortwave radiation reaching the surface and the outgoing longwave radiation, their accurate prediction is very important for daily weather forecasts and climate predictions. More detailed analyses of the results of the three-dimensional simulations on the fog and low-level clouds are being made, and will be reported elsewhere in the near future.

Acknowledgements

RSM forecasts, NEAR–GOOS daily SST products, and GMS-5 images were obtained from JMA. QuikSCAT data were downloaded from the anonymous ftp site of the National Aeronautics and Space Administration. The present study was performed through Research Revolution 2002 (RR2002) of Project for Sustainable Coexistence of Human, Nature and the Earth of the MEXT of the Japanese Government. A sample program of the improved M–Y Level-3 model is available at http://www.nda.ac.jp/~naka/MYmodel/.

References

Galperin, B., Kantha, L. H., Hassid, S., and Rosati, A.: 1988, 'A Quasi-Equilibrium Turbulent Energy Model for Geophysical Flows', *J. Atmos. Sci.* **45**, 55–62.

Gerrity, J. P., Black, T. L., and Treadon, R. E.: 1994, 'The Numerical Solution of the Mellor–Yamada Level 2.5 Turbulent Kinetic Energy Equation in the Eta Model', *Mon. Wea. Rev.* **122**, 1640–1646.

Helfand, H. M. and Labraga, J. C.: 1988, 'Design of a Nonsingular Level 2.5 Second-Order Closure Model for the Prediction of Atmospheric Turbulence', *J. Atmos. Sci.* **45**, 113–132.

Janjić, Z. I.: 2001, *Nonsingular Implementation of the Mellor–Yamada Level 2.5 Scheme in the NCEP Meso Model*, Office Note No. 437, National Centers for Environmental Prediction, 61 pp.

Japan Meteorological Agency.: 2002, *Outline of the Operational Numerical Weather Prediction at the Japan Meteorological Agency*, Appendix to the WMO Numerical Weather Prediction Progress Report, Japan Meteorological Agency, Tokyo, 158 pp.

Kantha, L. H. and Clayson, C. A.: 1994, 'An Improved Mixed Layer Model for Geophysical Applications', *J. Geophys. Res.* **99**(C12), 25235–25266.

Katayama, A.: 1972, *A Simplified Scheme for Computing Radiative Transfer in the Troposphere*, Numerical Simulation of Weather and Climate, Technical Report No. 6, University of California, Los Angeles, 77 pp.

Klemp, J. B. and Durran, D. R.: 1983, 'An Upper Boundary Condition Permitting Internal Gravity Wave Radiation in Numerical Mesoscale Models', *Mon. Wea. Rev.* **111**, 430–444.

Mellor, G. L. and Yamada, T.: 1982, 'Development of a Turbulence Closure Model for Geophysical Fluid Problems', *Rev. Geophys. Space Phys.* **20**, 851–875.

Musson-Genon, L.: 1987, 'Numerical Simulation of a Fog Event with a One-Dimensional Boundary Layer Model', *Mon. Wea. Rev.* **115**, 592–607.

Nakanishi, M.: 2000, 'Large-Eddy Simulation of Radiation Fog', *Boundary-Layer Meteorol.* **94**, 461–493.

Nakanishi, M.: 2001, 'Improvement of the Mellor–Yamada Turbulence Closure Model Based on Large-Eddy Simulation Data', *Boundary-Layer Meteorol.* **99**, 349–378.

Nakanishi, M.: 2002, 'A Lateral Boundary Condition Suitable for the One-Way Nesting Scheme', *Tenki* **49**, 117–128 (in Japanese).

Nakanishi, M. and Niino, H.: 2004, 'An Improved Mellor–Yamada Level-3 Model with Condensation Physics: Its Design and Verification', *Boundary-Layer Meteorol.* **112**, 1–31.

Smagorinsky, J., Manabe, S., and Holloway, J. L.: 1965, 'Numerical Results from a Nine-Level General Circulation Model of the Atmosphere', *Mon. Wea. Rev.* **93**, 727–768.